Inorg. Chem. **2003**, *42*, 8081–8086

Formation of Crystalline Stibnite Bundles of Rods by Thermolysis of an Antimony(III) Diethyldithiocarbamate Complex in Ethylene Glycol

Changhua An, Kaibin Tang,* Qing Yang, and Yitai Qian

Structure Research Laboratory and Department of Chemistry, University of Science and Technology of China, Hefei 230026, People's Republic of China

Received May 18, 2003

A synthesis of novel crystalline stibnite (Sb_2S_3) submicrometer-sized rod bundles of straw has been investigated using a wet chemical method via thermal decomposition of an antimony(III) diethyldithiocarbamate complex in ethylene glycol under mild conditions. By carefully controlling the experimental parameters, such as precursor concentration, temperature, and time, flowerlike bunches of rods and straw-shaped crystalline stibnite submicrometer-sized rod bundles are successfully achieved. The possible mechanism is proposed, which reveals that the inherent highly anisotropic layered structure of stibnite and precursor concentration take crucial roles in determining the final morphologies of the products. The high yields, simple reaction apparatus, low manipulating temperature, and newly discovered uniform morphology of the products may mean that this simple method has good potential in related future applications.

Introduction

In recent years, the synthesis of materials with specific morphologies such as rodlike, whiskerlike, and platelike, has been the current focus due to their special properties which have potential applications in molecular-based electronic devices such as optimal memory and switches, displays, and data records.[1] Especially, one-dimensional (1D) nanostructures including nanorods, nanowires, and nanotubes as building blocks for many novel functional materials are currently the focus of considerable interest.[2] So the synthesis of well-defined complex architectures based on nanorods or micrometer-sized rods would provide the opportunity to exploit the distinctive optical and electronic properties of the discrete 1D nanostructures and the possibility to probe potential new phenomena arising from their 2D or 3D organization.[3] There have been some attempts to synthesize complex architectures on the basis of 1D nanostructures. Alivisators and co-workers first reported a thermal decomposition approach using organometallic precursors to synthesize teardrop-, arrow-, and tetrapod-shaped CdSe nanocrystals.[3a] WS_2 nanotube bundles were prepared by R. Tenne et al. by employing a fluidized-bed reactor (FBR) route at relatively high temperature.[3c] The multiarmed CdS and MnS nanorods were prepared by Jun and co-workers in a monosurfactant system.[3b,d] Zhao et al. proposed a one-step surfactant ligand coassisted solvothermal method to produce multiarmed CdS nanorods.[4] 1D silica, Au, and Pt nanowire bundles and carbon nanotube bundles have also been reported by different authors.[5] However, the development of facile, mild, and effective methods for creating novel architectures based on nanorods or submicrometer-sized rods still remains a key scientific challenge.

The technological importance of antimony trisulfide (stibnite) is ascribed to its applications in television cameras,[6] microwave devices,[7] switching devices,[8] and various optoelectronic devices.[9] Owing to its good photoconductivity, it

* Author to whom correspondence should be addressed. E-mail: kbtang@ustc.edu.cn. Fax: 86-551-3601600.

(1) (a) Pan, Z. Y.; Liu, X. J.; Zhang S. Y.; Shen, G. J.; Zhang, L. G.; Lu, Z. H.; Liu, J. Z. *J. Phys. Chem. B* **1997**, *101*, 1973. (b) Vossmeyer, T.; DeIonno, E.; Heath, J. R. *Angew. Chem., Int. Ed. Engl.* **1997**, *36*, 1080. (c) Ohara, P. C.; Heath, J. R.; Gelbart, W. M. *Angew. Chem., Int. Ed. Engl.* **1997**, *36*, 1078.

(2) (a) Gudiksen, M. S.; Lauhon, L. J.; Wang, J.; Smith, D. C.; Lieber, C. M. *Nature* **2002**, *415*, 617. (b) Sun, Y.; Xia, Y. *Nano Lett.* **2002**, *2*, 165. (c) Yang, P.; Yan, H.; Mao, S.; Russo, R.; Saykally, R.; Morris, N.; Johnny, J.; He, R.; Choi, H.-J. *Adv. Funct. Mater.* **2002**, *12*, 323.

(3) (a) Manna, L.; Scher, E. C.; Alivisatos, A. P. *J. Am. Chem. Soc.* **2000**, *122*, 12700. (b) Jun, Y. W.; Lee, S. M.; Kang, N. J.; Cheon, J. *J. Am. Chem. Soc.* **2001**, *123*, 5150. (c) Rosentsveig, R.; Margolin, A.; Feldman, Y.; Popovitz-Biro, R.; Tenne, R. *Chem. Mater.* **2002**, *14*, 472. (d) Jun, Y. W.; Jung, Y. Y.; Cheon, J. *J. Am. Chem. Soc.* **2002**, *124*, 615.

(4) Gao, F.; Lu, Q.; Xie, S.; Zhao, D. *Adv. Mater.* **2002**, *14*, 1537.

(5) (a) Wang, Z. L.; Gao, R. P. P.; Gole, J. L.; Stout, J. D. *Adv. Mater.* **2000**, *12*, 1938. (b) Yang, C. M.; Shen, H. S.; Chao, K. J. *Adv. Funct. Mater.* **2002**, *12*, 143. (c) Lopez, M. J.; Rubio, A.; Alonso, J. A.; Qin, L. C.; Iijima, S. *Phys. Rev. Lett.* **2001**, *86*, 3056.

(6) Cope, D. U.S. Patent No. 2175359, 1959.

10.1021/ic034534n CCC: $25.00
Published on Web 10/24/2003

is also regarded as a prospective material for solar energy.[10] Another function of Sb_2S_3 is that it can be used as a raw material for the synthesis of sulfoantimonates of antimony and related compounds.[11] It is reasonable that the availability of architectures based on the 1D stibnite microstructure will introduce new types of applications or enhance the performance of currently existing devices.

A wide range of methods including vacuum evaporation,[12] chemical reaction,[13] and thermal decomposition[14] have been developed for the synthesis of stibnite. Polygonal bulk tubular Sb_2E_3 (E = S, Se) crystals and stibnite nanorods were prepared via the solvothermal route by Xie et al. and Qian et al., respectively.[15] A precipitation method has been proposed by C. López to fabricate Sb_2S_3 inverted opals.[16] E. T. Samulski and co-workers used a one-step, ambient-temperature synthesis of Sb_2S_3 microspheres.[17] Our group has also prepared Sb_2S_3 nanowires via an ethylenediamine-mediated polyol synthesis route using $SbCl_3$ and S powder as starting materials.[18]

The use of thiocarbamates as the sulfur source is well established in vapor deposition systems and inorganic nanoparticle growth.[19] In this paper, we have demonstrated a simple and convenient route to the production of novel uniform strawlike crystalline stibnite submicrometer-sized rod bundles by thermal decomposition of an antimony(III) diethyldithiocarbamate complex in ethylene glycol solution at ambient pressure. The large number densities of the products make the technique suitable and interesting for large-scale production, which may be of importance for the industrial production of novel materials.

Experimental Section

Materials and Instruments. All the chemical reagents such as anhydrous $SbCl_3$, sodium diethyldithiocarbamate ($NaC_5S_2N\,H_{10}$), and ethylene glycol (EG) purchased from Shanghai Chemical Co. were A.R. grade. They were used as received without further purification. Elemental analyses (Sb and S) of the as-synthesized precursor and the obtained stibnite were carried out by traditional chemical analysis. Elemental antimony was determined through the potassium bromate volumetric method, and sulfur was analyzed via a common barium sulfate gravimetric analysis.[20] The CN and H elements of the precursor were measured on a VARIO ELIII (German) element analytical instrument. IR spectra were obtained on a Bruker Vector-22 FT-IR spectrometer from 4000 to 500 cm^{-1} at room temperature. The samples and KBr crystal were ground together, and the mixture was pressed into a flake for IR spectroscopy. The crystalline phase of the products was determined by X-ray diffraction (XRD) using a Japan Rigaku D/max γA X-ray diffractometer equipped with graphite-monochromatized Cu Kα radiation (λ = 0.154178 nm). The accelerating voltage was set at 50 KV, with 100 mA flux at a scanning rate of 0.06/s in the 2θ range of 10−70°. The morphology and size of the obtained samples were investigated using field emission scanning electronic microscopy (FE-SEM), carried out on a JEOL JSM-6700F microanalyzer, and scanning electronic microscopy (SEM), performed on an X-650 scanning electron microanalyzer. The samples were prepared by deposition of an aliquot of the samples on copper pieces. The selected area electronic diffraction patterns were taken with a Hitachi model H-800 transmission electron microscope, using an accelerating voltage of 200 kV. The sample for the measurement was dispersed in absolute alcohol with an ultrasonic generator, and then the solution was dropped onto copper grids coated with amorphous carbon films. X-ray photoelectron spectra were obtained on an ESCALAB MKII X-ray photoelectron spectrometer, using nonmonochromatized Mg Kα as the excitation source. Raman spectroscopy was performed on a Jobin Yvon HR800 spectrometer (Horiba group) using 514.5 nm as the excitation line.

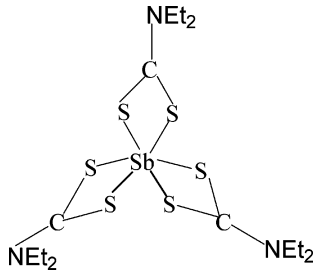

Figure 1. A scheme of the precursor structure.

Synthesis of the Antimony Diethyldithiocarbamate Complex. The antimony diethyldithiocarbamate complex was prepared from stoichiometric amounts of 0.1 mol·dm^{-3} $SbCl_3$ and 0.3 mol·dm^{-3} sodium diethyldithiocarbamate in absolute alcohol. The obtained yellow precipitate was filtered, washed with distilled water, and dried at room temperature. The reaction for the preparation of antimony(III) diethyldithiocarbamate can be formulated as follows:

$$SbCl_3 + 3Na(C_5S_2NH_{10}) \xrightarrow{\text{ethanol}} Sb(C_5S_2NH_{10})_3\downarrow + 3NaCl$$

The as-synthesized precursor was characterized by means of elemental analyses and IR spectroscopy. A scheme of the precursor structure is shown in Figure 1.

Synthesis of Bundles of Strawlike Stibnite Crystallites. In a typical procedure, 0.8 g of as-prepared Sb(III) diethyldithiocarbamate complex was placed in a round-bottomed flask with a

(7) Grigas, J.; Meshkanskas, J.; Orlimas, J. *Phys. Status Solidi A* **1976**, *37*, 10.
(8) Ablowa, M. S.; Andreev, A. A.; Deb Akaov, T. T.; Melekh, B. T.; Pautaow, A. B.; Sheridel, N. S.; Shirilona,L. N. *Sov. Phys. Semicond.* **1976**, *10*, 29.
(9) (a) Chokalingam, M. J.; Nagarajo Rao, K.; Rangavajan, R.; Suryanarayana, C. V. *J. Phys. D* **1970**, *3*, 1641. (b) Geroge, J.; Radhakrishnan, M. K. *Solid State Commun.* **1980**, *33*, 987.
(10) (a) Nair, M. T. S.; Nair, K.; Gancia, V. M.; Dena, Y.; Arenas, O. L.; Garcia, J. C.; Gomez-Daza, O. *Proc. SPIE-Int. Soc. Opt. Eng.* **1997**, *3138*, 186. (b) Savadogo, O.; Mondal, K. C. *Sol. Energy Mater. Sol. Cells* **1992**, *26*, 117.
(11) (a) Schimek, G. L.; Kolis, W.; Long, G. J. *Chem. Mater.* **1997**, *9*, 2776. (b) Stephan, H. O.; Kanatzidis, M. G. *Inorg. Chem.* **1997**, *36*, 6050.
(12) Ghosh, C.; Varmn, B. P. *Thin Solid Films* **1979**, *60*, 61.
(13) Carmalt, C. J.; Marison, D. E.; Parkin, I. P. *Main Group Met. Chem.* **1999**, *22*, 263.
(14) Lalia-Kantouri, M.; Manoussakis, G. E. *J. Therm. Anal.* **1984**, *29*, 1151.
(15) (a) Yang, J.; Zeng, J.; Yu, S.; Yang, L.; Zhang, Y.; Qian, Y. *Chem. Mater.* **2000**, *12*, 2924. (b) Zheng, X.; Xie, Y.; Zhu, L.; Jiang, X.; Jia, Y.; Song, W.; Sun, Y. *Inorg. Chem.* **2002**, *41*, 455. (c) Yang, Q.; Tang, K.; Wang, C.; Qian, Y.; Yu, W.; Zhou, G.; Li, F. *J. Mater. Chem.* **2001**, *11*, 257.
(16) Juárez, B. H.; Rubio, S.; Sánchez-Dehesa, J.; López,C. *Adv. Mater.* **2002**, *14*, 1486.
(17) Cheng B.; Samulski, E. T. *Mater. Res. Bull.* **2003**, *38*, 297.
(18) Shen, G. Z.; Chen, D.; Tang, K. B.; Jiang, X.; Qian, Y. T. *J. Cryst. Growth* **2003**, *252*, 350.
(19) (a) Trindade, T.; O'Brien, P. *Chem. Mater.* **1997**, *9*, 523. (b) Trindade, T.; O'Brien, P.; Zhang, X.; Motevalli, M. *J. Mater. Chem.* **1997**, *7*, 1011. (c) Monteiro, O. C.; Nogueira, H. I. S.; Trindade, T. *Chem. Mater.* **2001**, *13*, 2103.
(20) *Analysis of Rock and Mineral*, 1st Fascicule, 3rd Version; Geological Publishing Co.: Beijing, pp 188 and 486.

capacity of 500 mL. Then 45 mL of ethylene glycol was added, which was heated from room temperature to 290 °C. During the heating process, the complex was gradually dissolved in EG with an increase of temperature. After refluxing at 290 °C for 90 min, the flask was allowed to cool to room temperature naturally in air. The precipitates were rinsed with distilled water and absolute alcohol several times. After being dried in a vacuum at 50 °C for 2 h, the black powders were collected for characterization. In this reaction, EG may act as a nucleophilic solvent in the precursor decomposition process. Removal of the capping groups of antimony(III) diethyldithiocarbamate leads to the release of the inorganic [SbxSy] core, which can assemble into one-dimensional stibnite clusters. However, the identity of the byproducts formed during decomposition is still unknown. Further determination of the byproducts of the decomposition is under investigation.

Results and Discussion

Single-Source Precursor. The complex of antimony(III) diethyldithiocarbamate has not attracted much attention. A. H. White and co-workers first prepared and studied the crystal structure of the antimony(III) diethyldithiocarbamate complex.[21] L. Qu et al. investigated the synthesis of the complex using diethylamine, carbon disulfide, and antimony trioxide as raw materials. Its applications in poly(vinyl chloride) (PVC) resin as a heat stabilizer and in lithium complex grease as an extreme pressure antiwear agent were also studied.[22] Since anhydrous $SbCl_3$ hydrolyzes strongly in an aqueous solution, a nonaqueous solvent is used to synthesize the complex in our system. Meanwhile, owing to the good solubility of $Na(CS_2NEt_2)$ and $SbCl_3$ in ethanol, we chose nontoxic absolute alcohol as the solvent to prepare the antimony(III) diethyldithiocarbamate complex. When the $SbCl_3$/ethanol solution was added to the ethanol solution of $Na(CS_2NEt_2)$, a yellow precipitate immediately appeared, implying that antimony(III) diethyldithiocarbamate is formed in the solution. The elemental analysis and IR spectrum also confirmed the result.

Elemental analysis of the as-prepared precursor gives the Sb:S:N:C:H ratio as 1:5.5:2.6:14.8:29.2 for the antimony(III) diethyldithiocarbamate ($Sb(DDTC)_3$) complex, in agreement with the theoretical values within experimental error. The IR spectrum of the as-prepared Sb−DDTC complex is given in the Supporting Information. The characteristic absorption peaks at 1490 and 987 cm^{-1} can be undoubtedly assigned to the stretching vibrations of C−N and C−S, respectively.[19c] The peaks at 2868 and 2928 cm^{-1} may be assigned to ν_{C-H}. The deformation vibration C−H in $-CH_3$ and $-CH_2$ appears at 1354 and 1422 cm^{-1}.[22] At the same time, the frequency of the C−N stretching vibration of the complex shifted from 1477 cm^{-1} in pure Na(DDTC) (Figure 1b) to 1490 cm^{-1}. The shift of the C−N stretching vibration implies that the diethylthiocarbamate uses the sulfur atom to coordinate with the metal ion in the complex.[23] In other words, the overall characteristics of the IR spectrum of the as-prepared complex are basically consistent with the reported data for the Sb−DDTC complex reported by Qu et al.[22] From the results obtained from the elemental and IR analysis, we can confirm that $Sb(DDTC)_3$ is successfully prepared via the reaction of Na(DDTC) and $SbCl_3$ in absolute ethanol solvent.

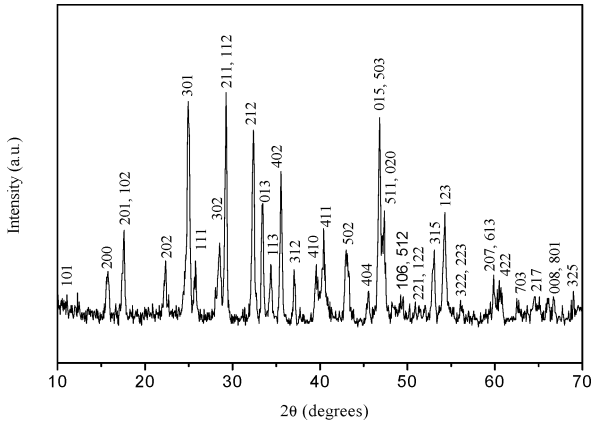

Figure 2. XRD pattern of the as-prepared strawlike stibnite crystals.

Characterization of Crystalline Stibnite Submicrometer-Sized Rod Bundles. Figure 2 shows a typical XRD pattern of the sample prepared from 0.8 g of precursor in 45 mL of EG at 290 °C for 90 min. All the diffraction peaks can be indexed to the orthorhombic unit cell of Sb_2S_3 with lattice parameters $a = 1.130$ nm, $b = 0.3834$ nm, and $c = 1.121$ nm, which are very close to the reported data (JCPDS Card 42-1393). No characteristic peaks of impurities, such as Sb_2O_3 or Sb, are detected in the pattern. Elemental analysis for the composition of the as-prepared product indicates that the target compounds are formed in a stoichiometric ratio, which is consistent with the analysis of XRD. The surface composition of the as-prepared product is further confirmed by X-ray photoelectron spectroscopy (XPS) as shown in Figure 3. The survey XPS spectrum of the product is illustrated in Figure 3A. The binding energies obtained in the XPS analysis are standardized for specimen charging using C1s as the reference at 284.6 eV. No peaks of other elements except Sb, S, and C are observed in the spectrum. Since the position of the Sb3d5 binding energy is superposed with the O2p binding energy, the Sb4d binding energy is taken for characterization. The characteristic peaks for Sb4d and S2p are at 33.96 and 162.1 eV, respectively (Figure 3B,C), which are close to the previously reported values.[24] The atomic ratio of Sb to S is estimated to be 2:2.89 by comparison of the integrated area for Sb4d and S2p, close to the results obtained from XRD and elemental analysis. Raman spectroscopy was also performed to further characterize the as-prepared strawlike stibnite crystal. As given in Figure 3D. The spectrum shows the typical Raman bands attributed to crystalline Sb_2S_3. The two peaks at 280 and 309 cm^{-1} can be assigned to the symmetric modes of the SbS_3 pyramid. The peak at 486 cm^{-1} may be attributed to

(21) Raston, C. L.; White, A. H. *J. Chem. Soc., Dalton Trans.* **1976**, 791
(22) Qu L.; Zhang M.; Li L.; Shu W. Y. *T. Nonferrous Met. Soc.* **1996**, *6*, 54.
(23) (a) Yamaguchi, A.; Penland, R. B.; Mizushima, S.; Lane, T. J.; Curran, C.; Quagliano, J. B. *J. Am. Chem. Soc.* **1958**, *80*, 527. (b) Swaminathan, K.; Irving, H. M. N. H. *J. Inorg. Nucl. Chem.* **1964**, *26*, 1291.
(24) Wanger, C. D.; Riggs, W. M.; Davis, L. E.; Moulder, J. F.; Muilenberg, G. E. *Handbook of X-ray Photoelectron Spectroscopy*: Perkin-Elmer Corp.: Eden Prairie, MN, 1978.

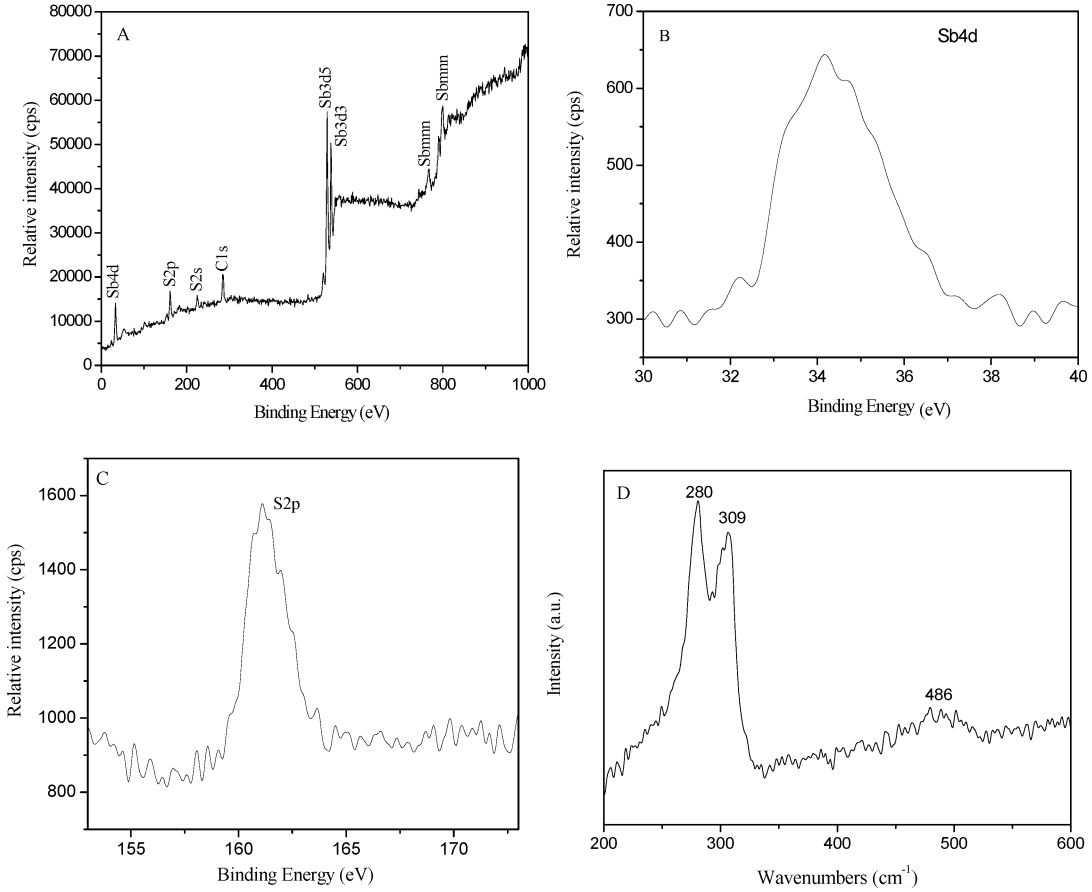

Figure 3. **(**A−C) XPS spectra of the same sample as analyzed in Figure 2: (A) survey data of the sample, (B) Sb4d core level spectrum, (C) S2p core level spectrum. **(D)** Raman spectrum of the same sample as examined in Figure 2.

the S−S vibration.[25,26] The results obtained from Raman spectroscopy of the as-prepared sample are similar to those for Sb_2S_3 inverted opals.[16]

The morphologies and microstructure of the products are investigated using FE-SEM. Figure 4A−D revealed the typical FE-SEM pictures of the same product as analyzed in Figure 2. These images indicate a large amount of submicrometer-sized rod bundles appears as a sheaf of straw tied in the middle, forming the strawlike microstructure of stibnite. The uniformity in the lateral dimension and their copiousness in quantity show a good growth environment for stibnite crystals in our system. By careful observation, each microcrystal is composed of numerous, highly aligned, and closely packed submicrometer-sized rods with uniform diameters (0.3−0.5 μm) and lengths (19−22 μm). Figure 4B gives an FE-SEM image of one typical stibnite crystal with one side facing us under higher magnification. We can observe that the crystalline stibnite bundles are made up of a lot of well-defined prismatic submicrometer-sized rods. Parts C and D of Figure 4 are higher resolution FE-SEM images, which also show the end of one stibnite microcrystal facing us.

At a given temperature and time (290 °C, 90 min), varying the precursor concentration results in controlling the shape of stibnite crystallites. Parts E and F of Figure 4 are SEM images of Sb_2S_3 grown at lower precursor concentration. As shown in Figure 4E, the stibnite obtained from a precursor concentration of 0.4 g in 45 mL of EG is mostly submicrometer-sized rod bunches with a flowerlike growth pattern. As the precursor concentration is increased to 0.6 g, an increase in the Sb_2S_3 submicrometer-sized rod bunches is observed (Figure 4F). To obtain a high yield of the bundlelike structured stibnite, a relatively high concentration of precursor (0.8 g) in the reaction solution is needed to enhance the nucleation and growth rate.

In the soft solution process, temperature and time are important factors influencing the yields of stibnite bundles of rods, which were proven in our contrast experiments. Typically, we chose the same sample investigated in Figure 2 as an example for systemic studies. Figure 5 shows SEM photographs of the products obtained at lower temperatures, keeping the other conditions identical. When the precursor is decomposed at 200 °C, the reaction is incomplete. The obtained product is composed of a small amount of bundles of rodlike crystals (Figure 5A). If the temperature is raised to 240 °C, the SEM image as shown in Figure 5B indicates the yield of bundles of rods increases in the sample. Higher energy input, provided by increasing temperature, may be contributed to self-assembly of the bundles of rods to yield strawlike bundles. As demonstrated in Figure 4A−D, a high yield of complete submicrometer-sized rod bundles of straw

(25) Mincera-Sukarova, B.; Najdoski, M.; Grozdanov, I.; chunnilall, C. J. J. *Mol. Struct.* **1997**, *410*−*411*, 267.
(26) El Idrissi Raghni, M. A.; Bonnet, B.; Hafid, M. L.; Oliver-Fourcade, J.; Jumas, J. C. *J. Alloys Compd.* **1997**, *260*, 7.

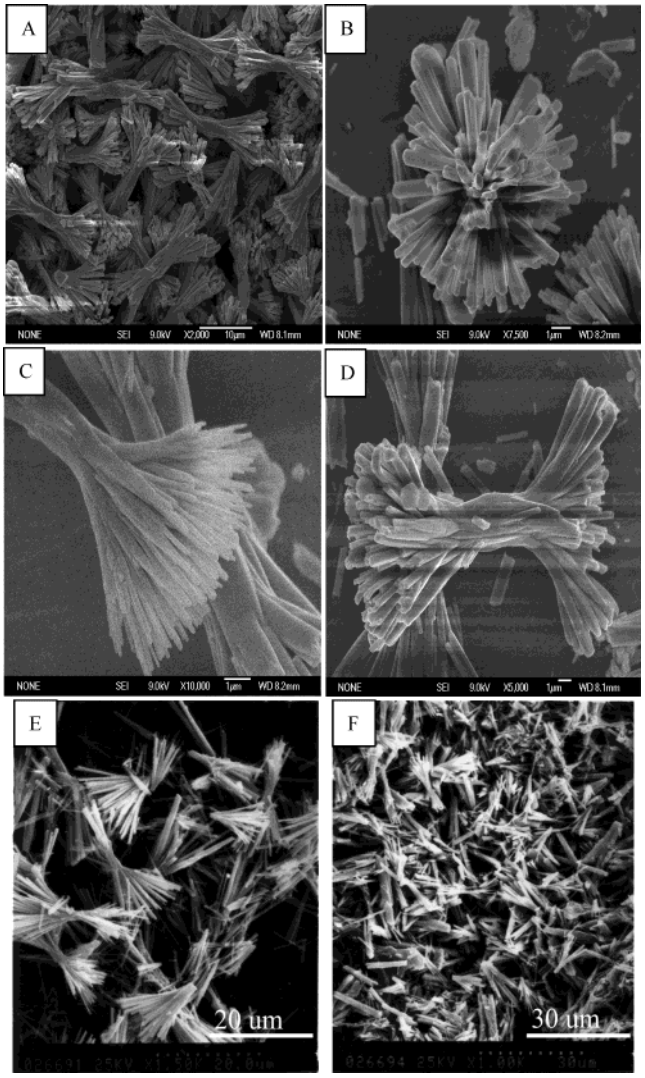

Figure 4. (A−D) FE-SEM images of the as-prepared strawlike stibnite crystals from 0.8 g of precursor in 45 mL of EG. (E, F) Change in the shape of the Sb_2S_3 microcrystals with changing precursor concentration at 290 °C for 90 min: (E) 0.4 g in 45 mL of EG, (F) 0.6 g in 45 mL of EG.

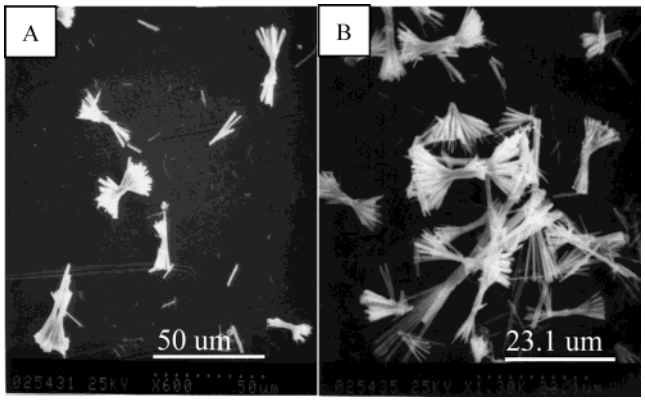

Figure 5. Evolution of stibnite crystals by variation of the growth temperature at a fixed time (90 min): (A) 200 °C, (B) 240 °C.

is successfully achieved with a temperature increase to 290 °C.

The stibnite crystals at various stages of the growth process are tracked by using SEM. Figure 6 shows a series of SEM images of the samples obtained at 290 °C after reaction for

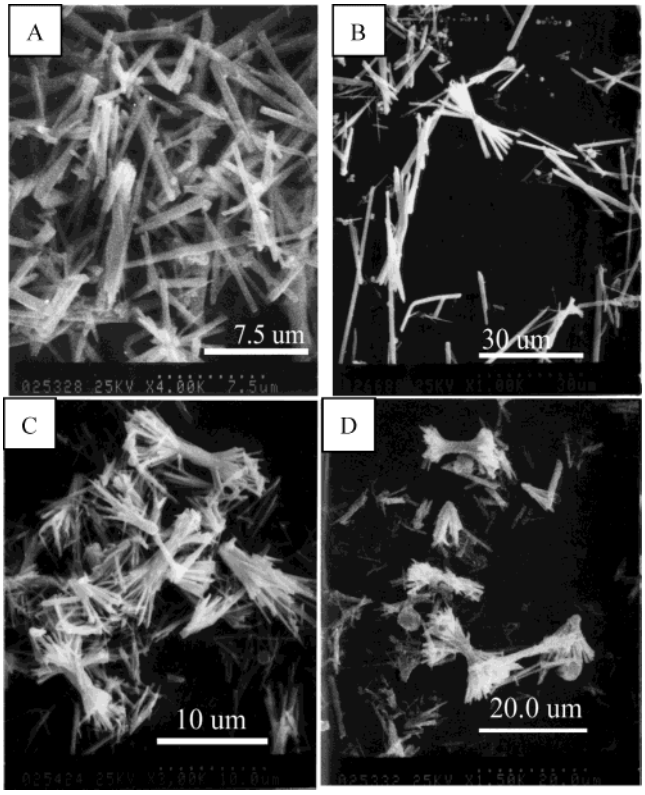

Figure 6. Time-dependent shape evolution of stibnite grown at 290 °C: (A) 10 min, (B) 20 min, (C) 30 min, (D) 40 min.

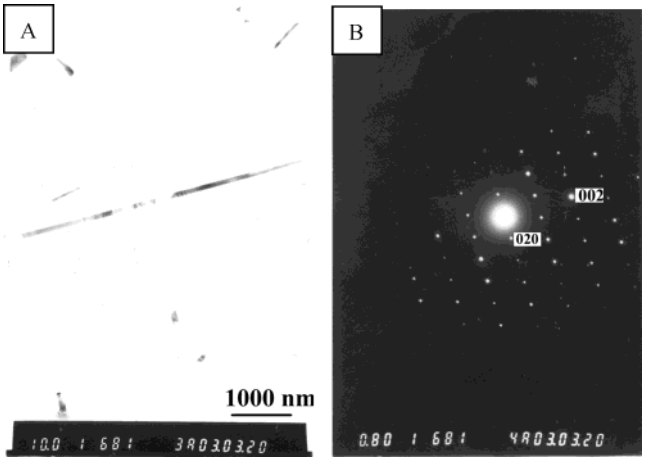

Figure 7. TEM photograph of stibnite nanorods synthesized at 290 °C for 10 min (A) and SAED pattern of a typical Sb_2S_3 nanorod (B).

10, 20, 30, and 40 min. These images show the evolution of stibnite crystals from 1D submicrometer-sized rods into the strawlike morphology over time at 290 °C. When the reaction proceeds for 10 min, the product is composed of rodlike crystals 0.1−0.3 μm in width and 7−10 μm in length, and some branched submicrometer-sized rods coexist. With an increase in time to 20 min, the prototype of bundles of rods appears initially. The sample obtained at 40 min (Figure 6D) indicates that the strawlike crystals with a length of ∼18 μm have been produced on a large scale. From the analysis of the above SEM images, it appears that the nucleation and growth is fast so that the fully grown bundles form very quickly (20−40 min). However, suitable a temperature and time are more favorable for the self-assembly process and

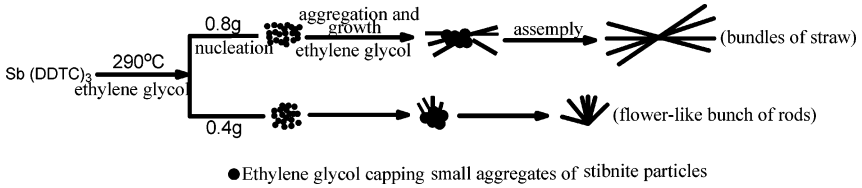

Figure 8. Schematic depicting possible growth routes for stibnite rod bunches and strawlike rod bundles.

provide more possibility for the nucleation and growth of a high yield of the uniform strawlike microstructure of stibnite crystals. This is demonstrated when the reaction is continued for 90 min.

Because the as-prepared crystalline stibnite bundles of straw are too thick to penetrate by an electron beam, we have used the sample synthesized at 10 min to further investigate the microstructure of stibnite crystals. Figure 7 presents a typical Sb_2S_3 nanorod 6 μm in length and 100 nm in diameter, and its corresponding selected area electron diffraction (SAED). The SAED pattern shows that it is a well-developed single crystal with growth direction along the *c*-axis, parallel to the (110) planes. The result is identical to the growth direction of Sb_2S_3 long crystals and nanorods reported by Xie et al. and Yang et al., respectively.[15a,b]

In the solution decomposition process, the effects of different solvents on the formation of stibnite crystals are also considered. When the $Sb(DDTC)_3$ complex is pyrolyzed in other solvents, such as ethylenediamine or ethanolamine, the stibnite crystals cannot be obtained. The sample prepared in glycerol is composed of some spherical particles and micrometer-sized rods on the basis of the observation of SEM images. Ethylene glycol, with appropriate velocity and coordination ability, may provide a good environment for the growth of stibnite bundles of rods. So, ethylene glycol is the optimal solvent for the production of crystalline stibnite bundles of rods in our experiments.

To understand the observed behavior of Sb_2S_3, it is necessary to study its structure. Stibnite is a highly anisotropic semiconductor with a layered structure parallel to the growth direction, and belongs to the orthorhombic system with space group D_{2h}.[16] It consists of infinite ribbonlike (Sb_4S_6) polymers, linked together by intermolecular attraction between antimony and sulfur atoms, which are parallel to the *c*-axis. The bonds within the ribbons are different in length owing to the two different types of coordination exhibited by both antimony and sulfur.[27] It is understandable that the crystallites, which nucleate along the *c*-axis, grow readily due to the inherent and unusual layered-type structure of stibnite, and thus the rodlike morphology formed. As for the formation of the bundlelike morphology, it is most probable that the nucleation of Sb_2S_3 occurs rapidly, which has been proven by our contrast experiments, and many newborn clusters agglomerate together to form small aggregates with ethylene glycol capping one particle surface more strongly, causing new Sb−S material to deposit on a particular particle face, and resulting in anisotropic growth. Then each of them starts to grow into rod crystals along the oriented direction (*c*-axis) when the clusters are in the excess saturation state. With the increase of temperature and time, flowerlike growth patterns of rodlike crystals finally result. Meanwhile, higher precursor concentrations can generate many more nucleation seeds at the tied region (Figure 4), and the growth fronts may radiate in stochastic opposite directions and lead to the formation of the strawlike rod bundles. The possible growth mechanism can be described diagrammatically in Figure 8. Of course, our present understanding of the formation mechanism for stibnite flowerlike rod bunches and strawlike rod bundles is still limited, and more in-depth studies are under way.

Conclusions

In summary, a soft solution process via thermal decomposition of the $Sb(DDTC)_3$ complex in ethylene glycol has been developed to prepare crystalline stibnite submicrometer-sized rod bundles of straw. If we discover how the oriented nucleation occurs in our system, we may be able to produce highly anisotropic microcrystals that could improve existing optical devices. The strawlike stibnite can be potentially converted to sulfoantimonates of antimony and related compounds with special morphology via the sacrificing template method. It is our hope that the present route may provide a general route to the synthesis of materials with complex architecture based on a one-dimensional microstructure and might be expanded to fabricate other materials with specific morphologies, such as As_2S_3, Bi_2S_3, MnS, and so forth.

Acknowledgment. This project is supported by the Chinese Natural Science Foundation, 973 Projects of China, State Key Project of Fundamental Research for Nanomaterials and Nanostructures, and Anhui Provincial Natural Science Foundation (Grant No. 03044901).

Supporting Information Available: Figure 1 shows the IR spectrum of the as-prepared Sb−DDTC complex. This material is available via the Internet at http://pubs.acs.org.

IC034534N

(27) (a) Mady, Kh. A.; Hammad, S. M.; Soliman, W. Z. *J. Mater. Sci.* **1987**, *22*, 4153. (b) Wells, A. F. *Structural Inorgnic Chemistry*; Clarendon Press: Oxford, 1975.